LA-UR-99-4137
Approved for public release; distribution is unlimited.

Title: **MATERIAL FAILURE AND PATTERN GROWTH IN SHOCK-DRIVEN ALUMINUM CYLINDERS AT THE PEGASUS FACILITY**

Author(s): John Stokes, R. D. Fulton, D. V. Morgan, A. W. Obst, D. M. Oro, H. Oona, W. Anderson E. A. Chandler and P. Egan

Submitted to:

http://lib-www.lanl.gov/cgi-bin/getfile?00796874.pdf

MATERIAL FAILURE AND PATTERN GROWTH IN SHOCK-DRIVEN ALUMINUM CYLINDERS AT THE PEGASUS FACILITY

John Stokes, R. D. Fulton, D. V. Morgan,
A. W. Obst, D. M. Oro, H. Oona, W. Anderson
Los Alamos National Laboratory, Los Alamos, New Mexico, USA
and
E. A. Chandler, P. Egan
Lawrence Livermore National Laboratory, Livermore, California 94551, USA

Abstract. Experiments on the Pegasus pulsed power facility have investigated material failure and the growth of sinusoidal perturbations machined on the free inner surface of both Al 1100 and Al 6061-T6 samples undergoing shocked acceleration. The material behind the free surface exhibits massive microspall resulting in a volume of low-density material. Rapid pattern growth in the failed material and subsequent pattern growth on the surface, including jetting in some cases, were seen. Shock pressures were 15 GPa and 50 GPa.

INTRODUCTION

Pegasus is a 4.2 MJ pulsed power machine used to implode a cylindrical liner 24 mm in radius and 0.4 mm thick in our experiments. The driving force is produced by the current flowing in the liner interacting with the magnetic field produced by the current. The pressure is proportional to the square of the magnetic field, which is proportional to the current times radius. We can vary this force by varying the charge on the capacitor bank.

The liner and target have been designed to produce a Taylor wave in the target to approximate the pressure wave from high explosive. This wave shape is triangular rather than a flat-toped shape which a flyer plate produces. Changing dimensions and driving current can vary the shock wave pressure profile. Pulsed power has the advantages that the grain structure effects of the explosive do not exist, and the driver is inexpensive relative to the cost of a uniform cylindrical explosive detonation. The Pegasus drive is highly symmetric, very reproducible and well diagnosed.

The diagnostic suite[1] available on Pegasus includes three to five radial and four axial x-ray images, a visible light image illuminated by a laser and/or self-emission, and various machine diagnostics [2] to measure the diving force. The radial x-rays are recorded on film, and the axial x-rays use a fluor with the images recorded on electronic cameras. All x-rays are independently timed. The backlighter and self-emission images are recorded on framing cameras.

Our experiments examined instabilities arising from the shock breakout in metals. Various effects, including inertial instabilities, elastic-to-plastic transition, material failure, and phase transitions contribute to the complex behavior in metals. Aluminum (Al) was chosen to avoid phase transitions at the pressures studied and to enable good radiography.

DISCUSSIONS OF THE EXPERIMENTS

The targets used in this study consisted of a cylinder shell of poly methyl methacrylate (PMMA) 2 mm thick, 17.5 mm long, with a 30 mm outer diameter. Lining the inside of the PMMA was an aluminum cylinder 3 mm thick and 17.5 mm long.

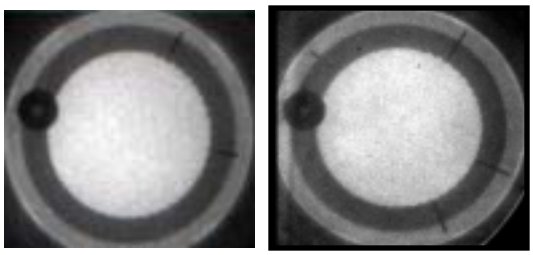

FIGURE 1 Preshot axial x-ray image of 6061 and 1100 Al targets. The small dark circle at about 10 o□clock is a brass fitting for gas injection.

Inside the aluminum was one atmosphere of either xenon or argon gas. Endcaps were made of PMMA 12 mm thick. Perturbations in the azimuthal direction are machined on the inside of the aluminum. We studied the effects of shock pressure and yield strength of material on spall and on the growth of these perturbations.

One pair of experiments examined the effect of yield strength on spall and growth of instabilities. Both targets had perturbations of 8¡ (1.396 mm) wavelength and amplitudes of 0.06 and 0.12 mm. One half of the inner circumference of each Al target was unperturbed and the different amplitudes were imposed on roughly 1/4 of each circumference. The target on the left in Fig. 1 was 6061-T6 aluminum. Inside the aluminum was 1 atm of xenon gas. The right-hand side of Fig. 1 was 1100-O aluminum with 1 atm of argon gas inside. This target had the same perturbations as the 6061 Al plus an additional perturbation of 6¡ wavelength and amplitude of 0.06 mm. A 120¡ sector of ultra-pure aluminum was also put in the unperturbed region in the lower left-hand corner.

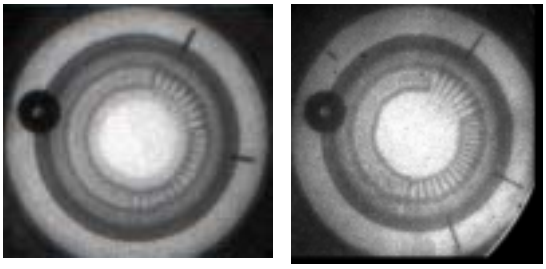

FIGURE 2. Dynamic axial x-ray images of 6061 and 1100 Al targets at 14 GPa shock pressure. From the center outwards the regions are unshocked gas (bright), shocked xenon (left picture only), spalled aluminum (dark ring), low-density aluminum, spalled aluminum (dark ring), low-density aluminum, normal density aluminum (outermost dark region), and PMMA.

Figure 2 shows axial dynamic radiographs of these two experiments at about the same time. The times of the x-ray pictures are 3.38 and 3.66 □s after liner collides with the PMMA. The shock pressure in these two experiments was 14 GPa. At this pressure, and also at 30 Gpa in a higher pressure experiment described separately [1], the spall structures are the same and show two distinct spall layers with lower-density regions outside each. Inside the inner spall layer one can see the shocked xenon in the 6061 aluminum experiment (left). The large perturbations were unstable in both experiments, while the smaller perturbations seemed to form a crust. There appears to be no large effect due to the difference in yield strengths in the two aluminum alloys. Their yield strengths [3] are 0.04 GPa for 1100 aluminum and 0.29 GPa for 6061 aluminum. However, the innermost crust of the 1100 Al appears to be slightly thinner than the innermost crust of the 6061 Al.

The primary purpose of the experiment was to see whether a yield strength 7 to 8 times smaller, as in AL 1100-O, would affect the stability of the perturbations. Yield strength plays a significant role in determining the growth of interfacial instabilities, such as Richtmeyer-Meshkov and Rayleigh-Taylor instabilities.

An issue that has been the subject of experiments in other geometries is the effect of grain size and impurities on spall strength [4]. To test the sensitivity of the microspall pattern to grain size we substituted a segment of 99.99% Al. This Al was in the 120¡ sector in the lower left corner of the right side of Figs. 1 and 2. This ultra-pure Al has larger grain sizes and fewer precipitates than the 1100 aluminum. The grains in the ultra-pure Al are millimeters longitudinally by 0.5 mm or more in cross-sectional diameter. Spall is thought to begin at void nucleation sites at grain boundaries and precipitates, and hence a difference might be expected in the spall structure. Instead we see that the spall in the region of ultra-pure Al has the same characteristics as the 1100 Al region. Figure 3 shows that more deviations from "circular" were observed later in time. This may reflect morphology, such as larger pieces of spall.

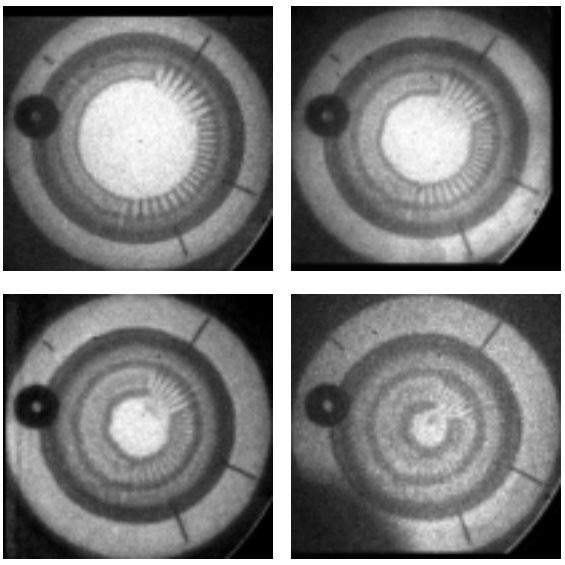

FIGURE 3. Dynamic axial x-ray images of the 1100 Al target with 99.99% Al 120¡ sector from the marker at 10:30 to 6:30 o□clock. Images were at 2.64 (upper left), 3.66 (upper right), 4.63 (lower left), and 5.37 □sec (lower right) after liner impact.

Figure 4 shows a radial x-ray view of the 6061 Al experiment shown axially on the left side of Fig. 2, and it is at the same time. We see the same microspall structure as seen axially. From the center to the left in fig. 4 we have unshocked xenon, shocked xenon, a spalled layer of Al, a lower density region, a second spalled layer of Al, another lower density region, the remaining aluminum, the

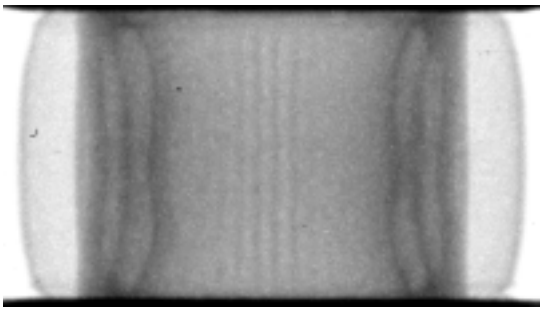

FIGURE 4. Dynamic radial x-ray images of the 6061 Al target shown in Fig.2 left side. From the center to left the regions are unshocked gas, shocked xenon, spalled aluminum (dark line), low-density aluminum, spalled aluminum (dark line), low-density aluminum, normal density aluminum, PMMA, and liner.

PMMA, and the liner. The center vertical stripes are the results of looking at the large amplitude perturbations machined into the aluminum. From this view we also see the end effects that we look through when we view the axial x-ray pictures. Note also that the outer Al is very straight showing that the liner was straight at impact. The bowing of the liner on the outside is due to end effects after impact.

A third experiment used 6061-T6 aluminum with the same 8¡-wavelength, 0.06-mm-amplitude perturbation as in the other 6061 aluminum target. A 24¡-wavelength perturbation with 0.06 mm amplitude replaced the large amplitude perturbation region of the target in Fig. 2. The gas on the inside was changed to argon at 1 atm for better contrast in the x-ray images. The shock pressure was increased to 50 GPa. Figure 5 shows that the 8¡ wavelength that was stable at 14 Gpa became unstable at 50 GPa. The growth of the 24¡-wavelength perturbation can easily be seen. Also notice that the character of the spalled layer in the unperturbed region is different. There are two distinct density regions of spall but no thin dense spalled layers, as were observed at 14 and 30 Gpa shock pressures.

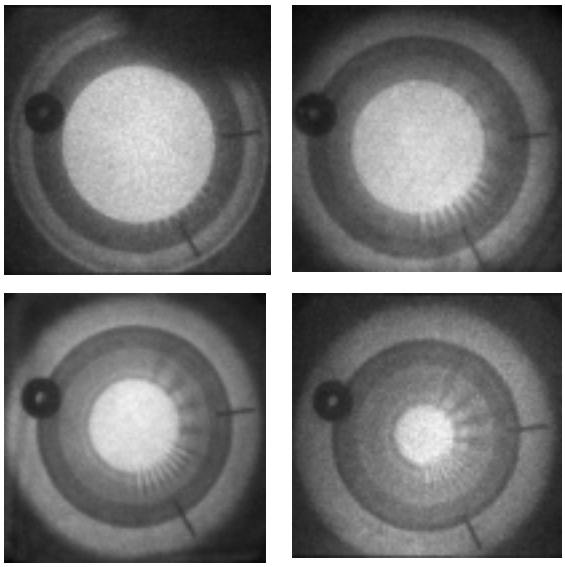

Figure 5. Dynamic axial x-ray images of 6061 Al target at 50 Gpa shock pressure. The images were at 0.90, 1.46, 2.07, and 2.68 □sec after liner impact.

SUMMARY

We have observed microspallation in three types of aluminum at pressures of 14-50 GPa. The general character of the spallation is independent of the yield strength of the aluminum alloys. At pressures of 14 and 30 GPa the spallation exhibited two spalled layers with lower density regions outside. When the pressure was increased to 50 GPa, the spall produced two different but uniform density regions. Evidence of a non-uniform spalled layer was seen in the time dependence of the ultra-pure aluminum spalled layer.

We have also studied the growth of small amplitude perturbations in both 1100 and 6061 aluminum at 14 GPa. The growth of these is also independent of yield strength. We also showed that the strength of the shock affects the stability of perturbation.

ACKNOWLEDGEMENTS

This work was performed under US DOE Contracts W-7405-ENG-48 and W-7405-ENG-36.

REFERENCES

1. Chandler, E. A., et al., "Use of Pegasus Z-Pinch Machine to Study Inertial Instabilities in Al: A Preliminary Report," in *Proc. of the 6th International Workshop on the Physics of Compressible Turbulent Mixing*, edited by G. Jourdan and L. Houas, Marseille, Impremerie Caractere, 1997, p. 111-115
2. Stokes, J. L., et al., "Precision Current Measurements on Pegasus II Using Faraday Rotation," in *Tenth IEEE International Pulsed Power Conference (Albuquerque, NM)*, edited by W. Baker and G. Cooperstein, IEEE, Piscataway, NJ, 1995, Vol. 1, pp. 378-383
3. Steinberg, D. J., "Equation of State and Strength Properties of Selected Materials," Lawrence Livermore National Laboratory, Livermore, CA, Tech. Rep. UCRL-MA-106439, 1996
4. Meyers, M. A., *Dynamic Behavior of Materials*, Wiley and Sons, New York, 1994, pp. 541-546